Reversible Fixation of Carbon Dioxide at Nickel(0) Centers: A Route for Large Organometallic Rings, Dimers, and Tetramers

Dirk Walther,* Christine Fugger, Heike Schreer, Rainer Kilian, and Helmar Görls[a]

Dedicated to Professor Ernst Anders on the occasion of his 60th birthday

Abstract: The reaction between bis(cycloocta-1,5-diene)nickel(0), carbon dioxide and benzaldehyde-*N*-furfurylideneimine (**A**) in 1,4-dioxane or THF results in the formation of the 24-membered organometallic macrocycles of the type $[(\mathbf{A})\mathrm{Ni(\text{-}CH(R^1)\text{-}N(R^2)\text{-}COO\text{-})}]_6(\mathrm{solv})_n$ (R^1: phenyl, R^2: furfurylidene, solv: 1,4-dioxane in **1a**, THF in **1b**). According to the X-ray analyses, six monomeric nickelacyclic units are connected through six Ni-μ_2-OCO-Ni bridges in these macrocycles. The cavities of the metallomacrocycles (diameter: 9.410(1) Å in **1a**, 9.250(1) Å in **1b**) each contain one solvent molecule. Reaction of **1b** with Me_3P results in the displacement of the peripheral ligands **A** by the phosphine to form the 24-membered organometallic macrocycle **1c**. Both **1a** and **1b** isomerize in benzene to form the dimeric complex $[(\mathbf{A})\mathrm{Ni(\text{-}CH(R^1)\text{-}N(R^2)\text{-}COO\text{-})}]_2(\mathrm{solv})_n$ (**2**). The X-ray crystal structure reveals that **2** consists of the same monomeric units as found in **1a** and **1b**. However two Ni-μ_2-O-Ni bonds link the carboxylato groups. The solvent-dependent isomerization of **1b** yielding **2** is a reversible reaction. Furthermore, the macrocycle **1b** partially eliminates carbon dioxide above 20°C, followed by elimination of half of the monodentately coordinated Schiff base ligands to form the planar tetrameric complex **6**. This is also a reversible process.

Keywords: carbon dioxide fixation · macrocycles · metallacycles · nickel · Schiff bases

Introduction

In most cases, the generation of metallamacrocycles by self-assembly reactions is based on reactions between metal ions and polydentate ligands and controlled by the information stored in the reactants. In contrast to this rapidly growing area of inorganic and coordination chemistry (for recent reviews see [1–6]), systematic investigations following the same principles for designing large *organometallic* rings containing transition metals which are intrinsic components of the organometallic macrocycle, are still rare.[7–9] A recent example for such a reaction is the synthesis of the interesting cyclic ferrocene oligomer containing seven ferrocene units.[10] Large "molecular squares" containing L_2Pt^{II} fragments connected by alkynediyl bridges can also be constructed.[11–13]

In this article we describe the synthesis, structure and reactivity of the macrocyclic organometallic molecules **1a**, **1b**, and **1c** via a complex synthetic approach. In the first step, we employ low-valent Ni centers in a redox template reaction in order to build up a new polydentate ligand from two simple molecules (CO_2/benzaldehyde-*N*-furfurylideneimine). In this step, the necessary square-planar geometry of the oxidized metal center Ni^{II} is generated for the subsequent step, that is the supramolecular aggregation forming the 24-membered organometallic rings **1a** (in 1,4-dioxane) and **1b** (in THF). Noteworthy the thermodynamically stable and kinetically inert carbon dioxide acts as the key building block in this reaction. These organometallic macrocycles undergo a variety of transformation reactions in which, surprisingly, the Ni–C bonds remain intact whereas the Ni–N, Ni–P, and Ni–O bonds can be easily broken. For example, **1b** isomerizes reversibly in benzene to form the dimer **2** by re-organization of the Ni–O bonds of the carbamato ligands. Another remarkable feature is the fact, that both **1a** and **1b** act as reversible CO_2 carriers which undergo carbon dioxide/Schiff base elimination to yield the tetrameric complex **6**. In addition, the two Ni-μ_2-O-Ni-bonds of the bridging Ni_2O_2 ring of **2** are cleaved by reaction with Me_3P or chelating ligands to form monomeric metallacycles (**3**–**5**). This highly flexible coordination behavior of the carbamato ligand may possibly be of interest for bioinorganic chemistry since carbamato groups are essential ligands in the active site of some metal-dependent enzymes (e.g., rubisco,[14] urease,[15] phosphatesterase,[16] biotin-depending enzymes[17]).

---

[a] Prof. Dr. D. Walther, Dr. C. Fugger, Dr. H. Schreer,
Dr. R. Kilian, Dr. H. Görls
Institut für Anorganische und Analytische Chemie
der Friedrich-Schiller-Universität Jena
August-Bebel-Strasse 2, 07743 Jena (Germany)
Fax: (+49) 3641-9-48102
E-mail: cdw@rz.uni-jena.de

0947-6539/01/0723-5214 $ 17.50+.50/0

Results and Discussion

Synthesis and solid state structure of the organometallic macrocycles 1a, 1b, and 1c: In order to obtain complex **1a**, [Ni(cod)$_2$] was mixed with an excess of the Schiff base benzaldehyde-*N*-furfurylideneimine (ligand **A**, see Scheme 1) (1:2.3) at ambient temperature in dioxane under argon and the mixture was stirred to form a dark violet solution. The argon was then substituted by dry gaseous carbon dioxide and a color shift to brown was observed. Compound **1a** crystallized from the reaction mixture in good yields (80%) as brown crystals upon addition of pentane. In addition, **1a** could be isolated in a more than 90% yield using [Ni^0(cdt)] as the starting product (cdt: cyclododeca-1.5.9-triene).

The nickel organic compound **1a** does not decompose at room temperature in the solid state as long as it is stored under argon or CO$_2$. It is also surprisingly stable when handled in air for a short time. The IR spectrum shows a characteristic asymmetric CO valence frequency at 1582 cm^{-1} and a typical C=N vibration at 1633 cm^{-1}.

The solid state structure of **1a** was determined by X-ray crystallography of single crystals grown from dioxane. Figure 1a displays the general molecular structure of the inner part of the complex. The same structure pattern was also found for the complexes **1b** and **1c** (L: benzaldehyde-*N*-furfurylideneimine for **1a**, and **1b**; L: Me$_3$P for **1c**). Figure 1b shows the complete structure of **1a**. Furthermore, Figure 2 contains the monomolecular unit and lists relevant bond lengths and bond angles in the legend.

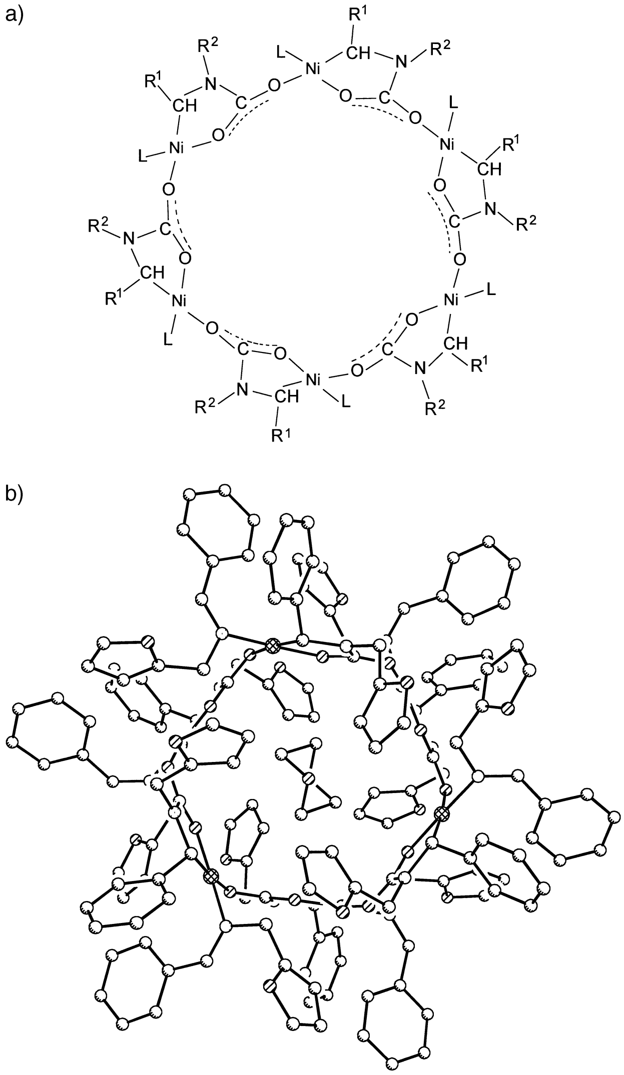

Figure 1. a) The structure of the inner part of the metalla-macrocycles **1a**–**1c** (R^1: phenyl, R^2: furfurylidene-; **1a** and **1b**: L = benzaldehyde-*N*-furfurylideneimine, **1c**: L = Me$_3$P; encapsulated solvent molecules are omitted for clarity). b) Molecular structure of the metallamacrocycle **1a**.

The crystal structure shows the organometallic complex to have a macrocyclic structure composed of six Ni^{II} centers, six carbon dioxide molecules, and twelve Schiff base ligands **A** (benzaldehyde-*N*-furfurylideneimine). Six of the ligands take part in the formation of six oxidative coupled slightly puckered five-membered NiOCNC chelate rings which also contain CO$_2$ molecules and the Schiff bases. Each Ni center lies approximately in the plane formed by a square which is bonded to the Schiff base nitrogen, two oxygen atoms of two carboxylato groups and the carbon atom of the oxidative coupling product between Schiff base and carbon dioxide. The bond lengths lie within the range usually observed for Ni–OCO and Ni–C bonds in metallacyclic complexes.[18, 19] The Ni $\cdots$ Ni separations (5.080(1) Å) clearly show that there is no bonding between the metals.

The six molecular units are connected by μ_2-OCO groups and yield a 24-membered macrocycle. Its cavity has an average diameter of 9.410(1) Å. One dioxane molecule which does not interact with the nickel centers is encapsulated in the inner part of the ring which is exclusively formed by the inorganic components Ni and the CO$_2$ unit (Figure 1). In addition, three dioxane molecules surround the macrocycle in

Abstract in German: *Die Reaktion zwischen Bis(cycloocta-1,5-dien)nickel(0), Kohlendioxid und Benzaldehyd-N-furfurylidenimin (**A**) in THF oder Dioxan führt zu 24-gliedrigen organometallischen Macrocyclen des Typs [(**A**)Ni(-CH(R^1)-N(R^2)-COO-)]$_6$(solv)$_n$ (R^1: phenyl, R^2: furfuryliden, solv: Dioxan in **1a**; THF in **1b**). Nach Ausweis der Röntgenstrukturanalysen sind in den Macrocyclen sechs monomere nickelacyclische Einheiten (**A**)Ni(-CH(R^1)-N(R^2)-COO-) durch sechs Ni-μ_2-OCO-Ni-Brücken verknüpft. Die Hohlräume des Metallamacrocyclen (Durchmesser: 9.410(1) Å in **1a**; 9.250(1) Å in **1b**) enthalten ein Lösungsmittel Molekül. Die Reaktion von **1b** mit Me$_3$P führt unter Verdrängung der peripheren Liganden **A** zum 24-gliedrigem organometallischen Macrocyclus **1c**. Die Verbindungen **1a** und **1b** isomerisieren in Benzol unter Bildung des dimeren Komplexes [(**A**)Ni(-CH(R^1)-N(R^2)-COO-)]$_2$(solv)$_n$ (**2**). Die Kristallstrukturanalyse zeigt, dass **2** aus den gleichen Monomeren wie **1b** besteht, allerdings verknüpft über Ni-μ_2-O–Ni Bindungen der Carboxylatogruppen. Die lösungsmittelabhängige Isomerisierung **1b** zu **2** ist eine reversible Reaktion. Die Verbindung **1b** eliminiert oberhalb 20°C einen Teil des Kohlendioxids. Nachfolgende partielle Eliminierung der einzählig gebundenen Schiffschen Base führt dann zum planaren tetrameren Komplex **6**. Das ist ebenfalls eine reversibler Prozess.*

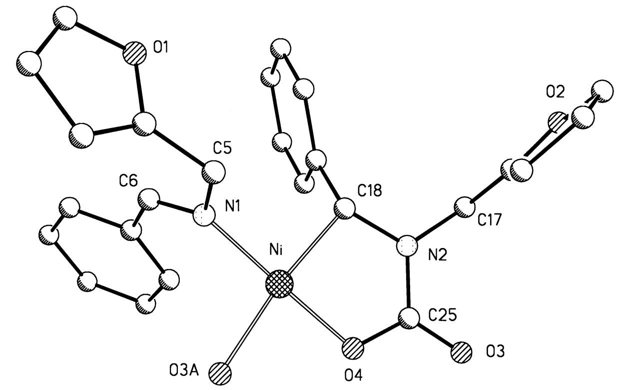

Figure 2. Molecular structure of the asymmetric unit of complex **1a** and **1b**. Selected bond lengths [Å] and bond angles [°] for **1a**: Ni–N1 1.896(2), Ni–O4 1.869(2), Ni–O3A 1.984(2), Ni–C18 1.935(2), N1–C5 1.500(3), N1–C6 1.288(3), N2–C17 1.459(3), N2–C18 1.477(3), N2–C25 1.361(3), C25–O3 1.272(3), C25–O4 1.292(3), N1-Ni-O3A 94.25(7), N1-Ni-O4 177.97(7), N1-Ni-C18 92.32(8), O3A-Ni-O4 87.53(6), O3A-Ni-C18 173.20(8), O4-Ni-C18 85.93(8), Ni-C18-N2 105.6(1), C18-N2-C25 116.9(2), N2-C25-O4 115.6(2), C25-O4-Ni 115.8(1), O4-C25-O3 124.0(2), C5-N1-C6 118.1(2); **1a**: Ni–Ni (neighboring) 5.080(1), Ni–Ni (diameter) 9.410(1); **1b**: Ni–Ni (neighboring) 5.007(1), Ni–Ni (diameter) 9.250(1); symmetry transformations used to generated equivalent atoms (A): $x-y, x, -z-2$. Selected bond lengths [Å] and bond angles [°] for **1c** (L = PMe_3 instead of L = **A**): Ni–P1 2.176(2), Ni–O4 1.888(4), Ni–O3A 1.951(2), Ni–C18 1.966(6), N2–C17 1.454(8), N2–C18 1.481(8), N2–C25 1.347(8), C25–O3 1.274(7), C25–O4 1.291(7), P1-Ni-O3A 92.4(1), P1-Ni-O4 178.1(1), P1-Ni-C18 95.9(2), O3A-Ni-O4 86.0(2), O3A-Ni-C18 170.6(2), O4-Ni-C18 85.6(2), Ni-C18-N2 104.7(4), C18-N2-C25 117.3(5), N2-C25-O4 116.8(5), C25-O4-Ni 115.0(4), O4-C25-O3 123.3(6); **1c**: Ni–Ni (neighboring) 4.962(1), Ni–Ni (diameter) 9.263(1); symmetry transformations used to generated equivalent atoms (A): $y+1, -x+y+1, -z+1$.

the crystal and also do not interact with the organometallic complex.

When the same reaction between [Ni(cod)$_2$], benzaldehyde-*N*-furfurylideneimine, and CO_2 was carried out in THF, cyclic hexamer **1b** was formed. Depending on the reaction conditions, compound **1b** crystallized with either four or six molecules of THF which may be partly removed in vacuo. The X-ray crystallography of single crystals grown from THF shows that the product has essentially the same macrocyclic structure as **1a**; the diameter of the cavity of the one THF molecule including macrocycle **1b** was found to be a bit smaller (9.250(1) Å) than that in **1a**. In contrast to the dioxane containing molecule **1a**, the THF encapsulated in the cyclohexamer **1b** creates an asymmetric situation in the cavity of the crystal. It was therefore not possible to determine the exact position of this THF molecule in the cavity by crystal structure analysis.

Both **1a** and **1b** show an interesting thermochromic effect. The orange red color of **1a** and **1b** in the solid state at room temperature turns to yellow green at −90 °C. This process is reversible. According to the X-ray crystallography, there is no significant difference in the structures of the 24-membered organometallic ring at both temperatures. Therefore we assume that this change of the color may depend on the rotation of the solvent molecules in the inner part of the cavities of **1a**, and **1b** which may be frozen at −90 °C.

The complexes (**1a** and **1b**) are also poorly soluble in both THF and dioxane. In benzene, a fast re-organization of **1a** and **1b** to form the dimer **2** takes place (see Scheme 1). Furthermore, both complexes dissociate into monomers by reaction with donor solvents and tend to eliminate CO_2. NMR measurements to determine the structure of both **1a** and **1b** in THF or dioxane thus failed. However, the solid state ^{13}C NMR spectrum of **1b** could be recorded. If all signals of the monomeric unit in **1b** (without signals for crystallizing THF) would be different from each other, one would expect 21 ^{13}C NMR signals with only three of them occuring below $\delta = 100$. In the solid state ^{13}C NMR spectrum of **1b**, 19 signals appear confirming that only one isomer crystallizes. Apart from the resonances of the olefinic and aromatic ^{13}C signals (between $\delta = 105.9$ and 151.7), three resonances appear at $\delta = 54.57$ (Ni–C), 42.23, and 39.71 (CH_2 of the furfuryl groups). As demonstrated by the X ray investigation, **1b** contains two different types of THF (either in the cavity of the macrocycle or in peripheral positions). Consequently, a double signal set for the ^{13}C atoms of THF at $\delta = 72.12/28.81$ and 66.49/24.72, respectively, was observed in the solid state ^{13}C NMR spectrum.

When a THF suspension of **1b** was allowed to stand at ambient temperature in the presence of Me_3P, the complex $[(Me_3P)Ni(\text{-}CH(R^1)\text{-}N(R^2)\text{-}COO\text{-})]_6(solv)_n$ (**1c**) was formed over a period of 2–4 d as indicated by the generation of a yellow solution. Complex **1c** was isolated in about 40% yield. An X-ray crystallographic study showed that **1c** also crystallizes with four molecules of THF and contains a very similar macrocyclic organometallic ring system as found for **1b**. The only difference is that Me_3P is bonded in peripheral positions instead of the monodendately coordinated Schiff bases in **1a** (Figure 1a). The diameter of the cavity which contains one THF molecule was found to be 9.263(1) Å, similar to organometallic macrocycle **1b**. Other selected bond lengths and angles are listed in the legend of Figure 2.

Synthesis and solid-state structure of the dimer 2: Whereas **1b** is only slightly soluble in THF, it can be readily dissolved in benzene to form an orange solution. Surprisingly, the orange dimeric compound **2** crystallizes in good yields (70%) at room temperature after a few hours from this solution (Scheme 1). Compound **2** was also obtained in an excellent yield (89%) by reaction of [Ni(cod)$_2$] with ligand **A** and CO_2 in benzene. The compound cocrystallizes with two benzene molecules both of which have no contact with the transition metal centers.

Scheme 1 shows the molecular composition of the dimer **2**, and Figure 3 displays the crystal structure of the compound. Relevant bond lengths and angles are listed in the legend. The

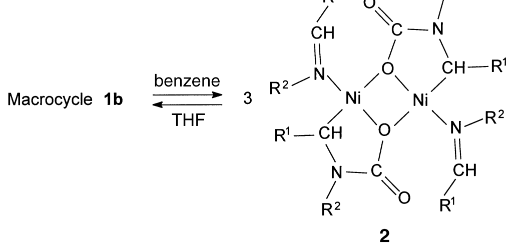

2

Scheme 1. Reversibility of the isomerization reaction and constitution of the dimer **2**. R^1: phenyl, R^2: furfurylidene.

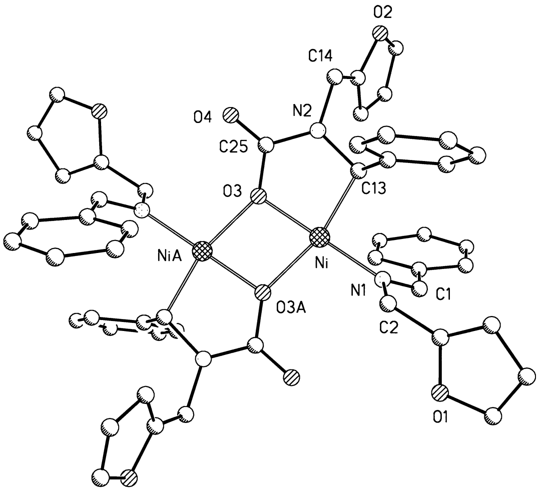

Figure 3. Molecular structure of complex **2**. Selected bond lengths [Å] and bond angles [°]: Ni–O3 1.864(2), Ni–O3A 1.983(2), Ni–N1 1.890(2), Ni–C13 1.924(2), N2–C13 1.474(3), N2–C14 1.452(3), N2–C25 1.363(3), C25–O3 1.332(3), C25–O4 1.228(3), N1–C1 1.289(3), N1–C2 1.495(3), N1-Ni-O3A 101.97(8), N1-Ni-O3 178.66(8), N1-Ni-C13 93.62(9), O3A-Ni-O3 78.25(8), O3A-Ni-C13 164.34(9), O3-Ni-C13 86.12(9), Ni-O3-NiA 101.74(8), Ni-C13-N2 105.1(2), C13-N2-C25 119.7(2), N2-C25-O3 111.7(2), C25-O3-Ni 116.8(2), C25-O3-NiA 140.9(2), O3-C25-O4 123.9(2), C1-N1-C2 119.2(2); Ni–Ni (neighboring) 2.985(1); symmetry transformations used to generated equivalent atoms (A): $-x+1$, $-y+2$, $-z+1$.

most interesting feature in this structure is that **2** consists of the same monomeric units as found in **1a**–**1c**. However, the coordination mode of the carboxylato groups is different.

In complex **2**, two monomeric units are linked by two Ni-O-Ni bonds thus yielding a dinuclear complex which contains a four-membered Ni_2O_2 ring. In contrast to this, Ni-μ_2-OCO-Ni bridges are exclusively formed in compounds **1a**–**1c** which leads to macrocyclic hexameric structures. Consequently, the Ni···Ni separation in **2** (2.985(1) Å) is much shorter than in the cyclic hexamers **1a**–**1c**. This difference in the coordination mode of the carbamato ligands also explains the shift in the CO valence frequencies observed (for example from 1582 cm^{-1} in **1b** to 1663 cm^{-1} in **2**).

Complex **2** was found to be stable in air for a short time. An orange solution is obtained, when dissolving the complex in THF, from which the cyclohexameric complex **1b** crystallizes after several hours in a good yield. This solvent-dependent reversible isomerization of **1b** to give **2** indicates, that there is only a small energy difference between the two coordination modes of the carbamato groups in **1b**, and **2**, respectively.

Why the cyclic compound **1b** is formed in THF whereas the formation of the dimer **2** is favored in benzene cannot be easily understood. However, it seems likely that the first step towards the formation of **1a**, **1b**, or **2** is the oxidative coupling of CO_2 with the Schiff base **A** at a low-valent Ni center [Ni^0(**A**)] to result in a monomeric species. This monomer may then react in different solvent-dependent aggregation reactions yielding either the cyclic hexamers **1a** (in THF), and **1b** (in 1,4-dioxane), or the dimer **2** (in benzene).

Additional evidence for a monomeric unit as the key intermediate for the formation of the isomers **1b** and **2** comes from the following reaction: When the dimeric compound **2** was reacted with an excess of Me_3P in THF, the Ni_2O_2 ring was cleaved which resulted in the monomeric complex [(Me_3P)(**A**)Ni(-CH(R^1)-N(R^2)-COO-)] (**3**) in which one Me_3P ligand stabilizes the monomeric unit (Scheme 2). Figure 4 shows the molecular structure of **3** and contains a list of selected bond lengths and angles.

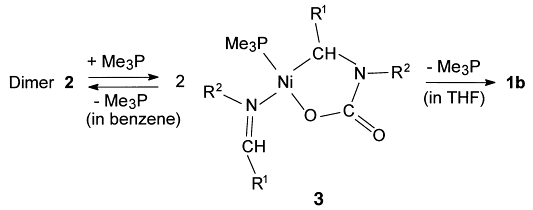

3

Scheme 2. Formation of the monomer **3** and solvent-dependent aggregation reactions upon elimination of Me_3P. R^1: phenyl, R^2: furfurylidene.

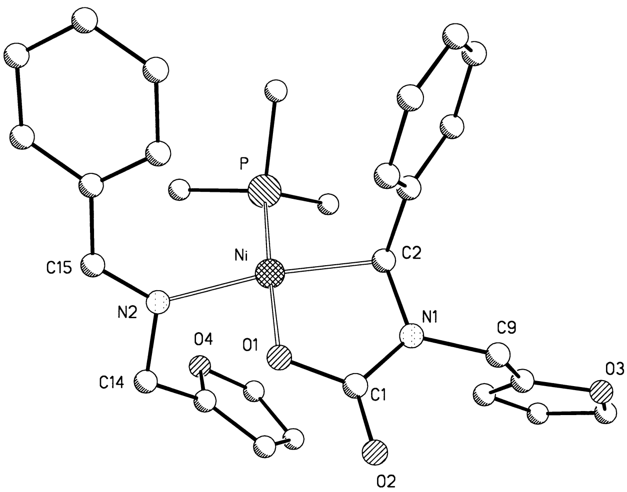

Figure 4. Molecular structure of complex **3**. Selected bond lengths [Å] and bond angles [°]: Ni–P 2.178(1), Ni–O1 1.886(4), Ni–N2 1.964(4), Ni–C2 1.953(5), O1–C1 1.317(7), O2–C1 1.238(7), N1–C1 1.369(7), N1–C2 1.476(6), N1–C9 1.454(7), N2–C14 1.483(7), N2–C15 1.296(7), P-Ni-N2 95.5(1), P-Ni-O1 176.4(1), P-Ni-C2 93.2(1), N2-Ni-O1 85.9(2), N2-Ni-C2 170.9(2), O1-Ni-C2 85.2(2), Ni-O1-C1 115.1(3), O1-C1-N1 113.3(5), O1-C1-O2 124.1(5), O2-C1-N1 122.6(5), C1-N1-C2 118.6(4), N1-C2-Ni 103.7(3), C14-N2-C15 115.3(4).

Upon solvation in THF, the monomer **3** eliminated trimethylphosphine when CO_2 was bubbled through the solution; this results in the formation of the cyclohexamer **1b** by aggregation of the monomeric unsaturated units. In benzene, however, the dimer **2** is formed from monomer **3** when Me_3P was eliminated in vacuo. Scheme 2 illustrates these reactions.

A monomerization of **1** or **2** can also easily be achieved when **1** or **2** are reacted with the chelating 2,2′-bipyridine (bpy), or *N,N,N′,N″,N″*-pentamethyldiethylenetriamine (ptmeda) ligands. Under these conditions, the monodentately coordinated Schiff bases were displaced and the bridging carboxylato groups were cleaved which resulted in the monomeric metallacyclic products **4** and **5**, respectively. These monomeric complexes can also be prepared from ligand **A**, CO_2, Ni^0 and bpy or ptmeda analogous to the formation of other oxidative coupling products.[20–22] Scheme 3

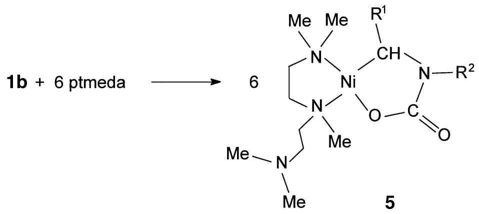

Scheme 3. Formation of complex **5**. ptmeda: *N,N,N′,N″,N″*-pentamethyldiethylenetriamine, R^1 = phenyl, R^2 = furfurylidene.

illustrates the formation reactions and shows the constitution for **5**.

The solid state structure of compound **5** determinated by X-ray crystallography demonstrates that ptmeda (a neutral N-N-N ligand) only acts as a bidentate ligand (Figure 5). The nickel(II) center is approximately square-planar and the carbamato group is monodentately coordinated. Additional bond lengths and angles are listed in the legend. Since these values lie within the range expected for such compounds they do not need further comments.

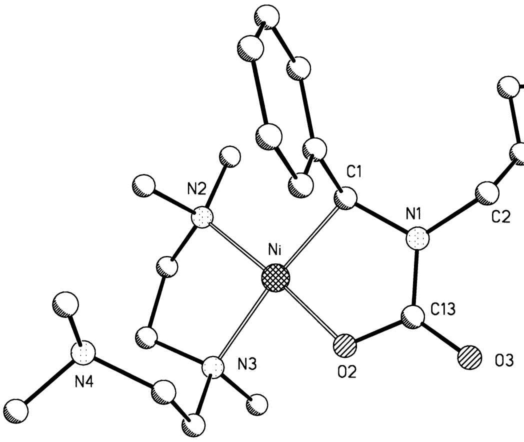

Figure 5. Molecular structure of complex **5**. Selected bond lengths [Å] and bond angles [°]: Ni–C1 1.941(3), Ni–O2 1.852(2), Ni–N2 1.966(2), Ni–N3 2.039(2), N1–C1 1.471(3), N1–C2 1.461(3), N1–C13 1.376(4), C13–O2 1.310(3), C13–O3 1.240(3), C1-Ni-O2 85.7(1), C1-Ni-N2 98.7(1), C1-Ni-N3 173.8(1), N2-Ni-N3 87.4(1), N2-Ni-O2 175.53(9), N3-Ni-O2 88.11(9), Ni-O2-C13 116.7(2), O2-C13-O3 124.1(3), O2-C13-N1 113.1(2), O3-C13-N1 122.8(3), C13-N1-C1 117.3(2), N1-C1-Ni 104.4(2).

Reversible CO_2 fixation and the structure of complex 6: In THF or benzene, complex **1b** undergoes an interesting partial elimination reaction of both CO_2 and Schiff base either in vacuo or at temperatures above 20 °C. Under these conditions, the organometallic tetramer **6** is formed which crystallizes from the THF solution as deep red crystals. The IR spectra show that the C=N band is shifted to higher values as compared with **1a**/**1b** (1648 cm^{-1}) whereas the CO band is unaffected ($\tilde{\nu}_{CO}$ = 1582 cm^{-1}).

The X-ray diffraction analysis of single crystals of **6** yielded a tetrameric structure in which all four Ni centers show an approximately square-planar geometry (Figure 6). Relevant bond lengths and angles are also listed in the legend.

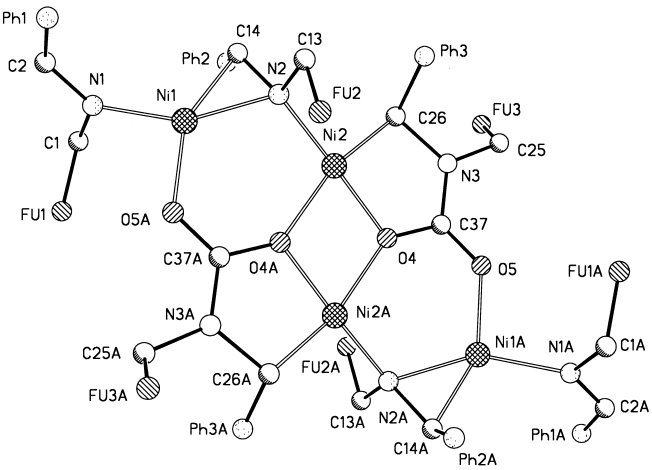

Figure 6. Molecular structure of complex **6**. Selected bond lengths [Å] and bond angles [°]: Ni1–N1 1.908(6), Ni1–C14 1.899(7), Ni1–N2 1.917(6), Ni1–O5A 1.957(5), Ni2–N2 1.879(5), Ni2–C26 1.924(7), Ni2–O4 1.861(4), Ni2–O4A 1.996(5), N1–C1 1.477(10), N1–C2 1.219(9), N2–C14 1.392(9), N2–C13 1.504(9), N2–C37 1.336(10), N3–C25 1.444(10), N3–C26 1.502(9), N3–C37 1.336(10), O4–C37 1.331(9), O5–C37 1.242(8), N1-Ni1-C14 107.0(3), N1-Ni1-N2 149.8(3), N1-Ni1-O5A 99.3(2), C14-Ni1-N2 42.8(3), C14-Ni1-O5A 152.4(3), N2-Ni1-O5A 110.7(2), C26-Ni2-O4 86.6(3), C26-Ni2-O4A 163.0(2), C26-Ni2-N2 99.1(3), O4-Ni2-O4A 77.3(2), O4-Ni2-N2 171.7(2), O4A-Ni2-N2 97.5(2), Ni2-O4-Ni2A 102.7(2), C1-N1-C2 117.0(7), Ni1-C14-N2 69.3(4), C14-N2-Ni1 67.9(4), Ni2-C26-N3 104.3(4), C26-N3-C37 119.1(6), N3-C37-O4 113.5(6), N3-C37-O5 123.2(8), C37-O5-Ni1A 120.2(5), C37-O4-Ni2A 141.3(4), Ni1–Ni2 3.155(1) Ni2–Ni2A 3.013(1). Symmetry transformations used to generated equivalent atoms (A): $-x+1$, $-y+1$, $-z$.

Complex **6** is very symmetrical and consists of a central dimeric unit and two peripheral monomeric units. Both peripheral metal centers are surrounded by two Schiff base ligands which have different coordination patterns (Figure 7). One Schiff base acts as a monodentate ligand and coordinates via the free electron pair on nitrogen as seen in **1** and **2**. The other Schiff base coordinates in an olefine-like coordination. In addition, the nitrogen forms a Ni-N-Ni bridge to the neighboring Ni^{II} atom of the inner unit. The bond lengths of the C–N bonds of the side on coordinating Schiff bases (1.392(9) Å) are those of single bonds.

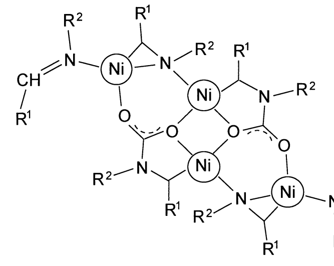

Figure 7. Different coordination patterns of Schiff base ligand **A** in complex **6**. R^1 = phenyl, R^2 = furfurylidene.

The environment of both inner Ni^{II} centers is very similar to that of the dimer **2** (Figure 2). The only remarkable difference is that the nickel-azirane ring of the peripheric fragment acts as an additional ligand in **6** instead of the monodentate Schiff base in complex **2**. As expected for this arrangement the Ni ··· Ni separations (Ni1–Ni2 3.155(1) Å, Ni2–Ni2A 3.013(1) Å) are significantly shorter than in the macrocycles **1a**–**1c**.

It is noteworthy that the conversion reaction **1b** to form **6** is a reversible reaction:

$$2 \times \text{complex } \mathbf{1b} \rightleftharpoons 3 \times \text{complex } \mathbf{6} + 6\,CO_2 + 6\,R^1\text{-CH=N-R}^2 \quad (1)$$

(R^1: phenyl, R^2: furfurylidene)

Dissolving the isolated tetramer **6** in THF in the presence of the Schiff base **A** and an excess of carbon dioxide results again in the formation of the hexameric compound **1b** which crystallizes from the solution. In other words, the macrocyclic complex **1b** acts as a reversible CO_2 carrier eliminating carbon dioxide/Schiff base **A** under mild conditions to form the tetramer **6** which is able to uptake CO_2 from a CO_2 atmosphere when additional Schiff base **A** is present.

The formation of the tetrameric compound **6** may start by CO_2 elimination from the cyclic metalla-carbamate **1b** yielding a nickel-azirane ring. The nitrogen atom of this ring acts as bridging ligand connecting the nickel-azirane ring with a cyclic nickel carbamate unit. Subsequent re-organization of these fragments resulting in the elimination of Schiff base and the formation of the tetramer **6** is a complex process which is as yet not well understood. During the formation of **6** the carbamato groups change their coordination mode from bidentate bridging ligands to tridentate ligands connecting three Ni centers.

The molecular structure of **6** may well provide deeper insight into the formation processes of the complexes **1** and **2**. It is likely that the Schiff base ligands in the tetramer **6**, having two different coordination modes may have different functions: Whereas the monodentately coordinated Schiff bases could possibly tune the CO_2 reactivity of the metal centers, the side-on bonded Schiff bases may act as a substrate for CO_2 as part of a metalla-azirane ring.

Conclusion

The formation of the large organometallic rings **1a** and **1b** from CO_2, Ni^0, and benzaldehyde-*N*-furfurylideneimine is a remarkable reaction which demonstrates the potential of organometallic basic reactions for self-assembling processes of large organometallic rings. Complex **1c**, the product of the reaction between **1b** and Me_3P, contains the same 24-membered ring as **1a**, and **1b**. The solvent-dependent isomerization of the complex **1b** to form **2**, and the CO_2 elimination from **1a**,**1b**, or **2** coupled with the elimination of benzaldehyde-*N*-furfurylideneimine ligands to form complex **6**, demonstrate that the carbamato complexes are higly flexible systems. These reactions are reversible. In addition, the X-ray structure of **6** is of general importance, because it provides deeper insight into the function of reversible CO_2 carriers based on Schiff bases R^1-CH=N-R^2 which reversibly uptake CO_2; that is provided that the Schiff bases are bonded to low-valent nickel in an olefine-like fashion. Furthermore, it is surprising that in all reactions studied here, the Ni–C bonds remained intact whereas the Ni–P, Ni–N and Ni–O bonds can be cleaved easily.

Moreover, the high flexibility of the coordination mode of the carbamate groups, which act as monodentate ligands in **3**, **4**, and **5**, as bidentate Ni-μ_2-OCO-Ni bridges in **1a**–**1c**, as bidentate Ni-μ_2-O-Ni bridging ligands in **2**, and as tridentate ligands connecting three Ni centers in **6**, is remarkable with respect to the function of such groups in enzymes containing carbamato ligands.

In this context, it is noteworthy that the coordination mode of the carboxylato groups in **1a**–**1c** is essentially the same as in the enzyme urease which contains a Ni_2 unit.[15, 23]

Experimental Section

General methods: All reactions were carried out under an argon atmosphere using a standard Schlenk technique. Solvents were dried using standard methods. THF was distilled from sodium/benzophenone immediately prior to use.

NMR spectra were obtained on a Bruker AC 200 MHz spectrometer and all spectra were referenced to TMS or deuterated solvent as an internal standard. The solid state NMR spectrum was obtained on a Bruker AMX 400 (100.6 MHz) spectrometer. FAB mass spectra were obtained on a Finnigan MAT SSQ 710 equipment (2,4-dimethoxybenzylalcohol as matrix). IR measurements were carried out on a Perkin Elmer System 2000 FT-IR.

Materials: Furfurylidene amine and benzaldehyde were distilled, kept, and handled under argon; benzaldehyde-*N*-furfurylideneimine was prepared from benzaldehyde and furfurylidenamine in toluene analogously to literature procedures.[24, 25] Pure CO_2 (4.8) from Linde AG are used without additional purification.

Compound 1a: Benzaldehyde-*N*-furfurylideneimine (0.88 g, 4.76 mmol) was added to a stirred solution of [Ni(cod)$_2$] (0.655 g, 2.38 mmol) in dioxane (25 mL) at room temperature. Subsequently the dark purple solution was treated with CO_2 at 20 °C for 2 h and the solution was stirred for additional 2 h. Pentane (25 mL) was added to the brown reaction mixture and cooled down to −20 °C. After 24 h, **1a** containing four dioxane molecules per macrocycle was obtained as orange-brown crystals. Single crystals of **1a**, also containing four dioxane molecules were grown from a dioxane/diethyl ether mixture (1:1). Yield: 1.0 g (80 %) for [**1a**·(1,4-dioxane)$_4$]; elemental analysis calcd (%) for $C_{166}H_{164}N_{12}Ni_6O_{32}$ (3191.4): C 62.47, H 5.38, N 5.27, Ni 11.04; found C 62.48, H 5.08, N 5.14, Ni 10.96; IR (nujol): $\tilde{\nu} = 1582$ (C=O), 1596 (C=C), 1633 (C=N) cm^{-1}; GC: 3.88 equiv, $C_4H_8O_2$/Ni$_6$ unit.

Compound 1b: Benzaldehyde-*N*-furfurylideneimine (0.88 g, 4.76 mmol) was added at room temperature to a stirred solution of [Ni(cod)$_2$] (0.655 g, 2.38 mmol) in THF (25 mL). After formation of a dark purple solution CO_2 was bubbled into the solution at −20 °C for 2 h yielding an orange-brown solution. Then the reaction mixture was allowed to warm to room temperature and stirred for 2 h at this temperature. Upon addition of diethyl ether (25 mL) the mixture was cooled to −20 °C. Compound **1b**, which crystallized with four THF molecules, was obtained as orange-brown crystals suitable for X-ray analysis. Yield: 0.65 g (58 %) for [**1b**·(THF)$_4$]; elemental analysis calcd (%) for $C_{166}H_{164}N_{12}Ni_6O_{28}$ (3127.48): C 63.75, H 5.28, N 5.34, Ni 11.32; found C 64.08, H 5.09, N 5.19, Ni 11.25; ^{13}C NMR (solid state, 100.6 MHz, 298 K): $\delta = 24.7$, 28.8 (CH$_2$, THF), 39.7, 42.2, (N-CH$_2$), 54.6 (Ni-C), 66.5, 72.1 (CH$_2$, THF), 105.8, 111.4 (C$_{\text{quart}}$), 123.2, 127.1, 129.7, 131.5 (CH=CH), 140.3, 146.0 (C$_{\text{quart}}$), 150.5, 151.8 (=CH-O), 166.9 (C=N), 168.6 (C=O); IR (nujol): $\tilde{\nu} = 1582$ (C=O), 1633 (C=N) cm^{-1}; MS(FAB): *m*/*z*: 473 [M/6]$^+$; GC: 4.3 equiv, THF/hexameric unit. The yield of **1b** can be improved to 90 % by using [Ni(cdt)] instead of [Ni(cod)$_2$].

Compound 1b (starting from **2**): A solution of **2** (2.35 g, 2.49 mmol) in THF (20 mL) was saturated with CO_2. The reaction mixture was stirred for 2 h, and to the resulting orange-brown solution diethyl ether (20 mL)was added. [**1b**·(THF)$_4$] was isolated at −20 °C as orange-brown single crystals suitable for X-ray analysis. Yield: 2.95 g (75 %).

Compound 1c: A suspension of [**1b**·(THF)$_4$] (1.84 g, 0.59 mmol) in THF (40 mL) was saturated with CO_2 at −40 °C. The reaction mixture was stirred for 30 min. After adding trimethylphosphine (370 μL) at −30 °C through a syringe the color of the mixture changed from orange-brown to yellow. After 6 h a yellow solution was formed. Diethyl ether (40 mL) was added, and **1c** was isolated at −20 °C after 2–4 d as a light yellow crystalline substance, crystallizing with four molecules of THF. Single crystals also containing four molecules THF/hexameric unit were grown from THF. Yield: 583 mg (40 %) for [**1c**$\cdot$(THF)$_4$]; elemental analysis calcd (%) for $C_{112}H_{152}N_6Ni_6O_{22}P_6$ (2472.59): C 54.41, H 6.20, N 3.40, P 7.52, Ni 14.25; found C 54.70, H 6.17, N 3.21, P 7.44, Ni 14.23; IR (nujol): $\tilde{\nu} = 1568$ (C=O), 1592 (C=C) cm^{-1}, MS(FAB): *m*/*z*: 364 [*M*/6]$^+$; GC: $t_R = 3.5$ min, THF/Ni$_6$ unit.

Compound 2: Benzaldehyde-*N*-furfurylideneimine (1.65 g, 8.90 mmol) was added under stirring at room temperature to a benzene solution (25 mL) of [Ni(cod)$_2$] (1.22 g, 4.45 mmol). The mixture was treated with CO$_2$ at 20 °C, and orange-brown crystals of **2** containing two benzene/dimeric unit were separated from the orange solution after stirring for 2 h. Single crystals of the same composition suited for X-ray crystallograpy were obtained by slow crystallization from dilute benzene solution. Yield: 1.87 g (89 %) for [**2**$\cdot$(benzene)$_2$]; elemental analysis calcd (%) for $C_{62}H_{56}N_4Ni_2O_8$ (1102.52): C 67.54, H 5.12, N 5.08, Ni 10.65; found C 67.04, H 5.26, N 5.16, Ni 10.44; IR (nujol): $\tilde{\nu} = 1579$, 1596 (C=C), 1633 (C=N), 1663 (C=O) cm^{-1}; MS(FAB): *m*/*z*: 473 [*M*/2]$^+$; GC: $t_R = 0.9$ min, C_6H_6/Ni unit.

Compound 3: A suspension of **2** (1.26 g 1.33 mmol) in THF (20 mL) was saturated with CO$_2$. The reaction mixture was stirred for 30 min. After adding trimethylphosphine (300 µL) at −30 °C through a syringe the color of the mixture changed from the orange-brown of the suspension to a yellow solution. After adding of diethyl ether (20 mL) **3** was isolated at −20 °C after 2–4 d as light yellow solvent free crystals. Single crystals of **3** containing two molecules of THF were grown from dilute THF solutions containing a small amount of diethyl ether. Yield: 322 mg (22 %); elemental analysis calcd (%) for $C_{28}H_{31}N_2NiO_4P$ (549.25): C 61.23, H 5.69, N 5.10, P 5.64, Ni 10.69; found C 61.00, H 5.72, N 4.92, P 5.50, Ni 10.77; IR (nujol): $\tilde{\nu} = 1582$ (C=O), 1598 (C=C), 1616 (C=N) cm^{-1}; ^{1}H NMR (298 K, 200 MHz, [D$_8$]THF): $\delta = 1.16$ (s, 9H, CH$_3$), 3.59 (s, 1H, CH-Ni), 4.73 (s, 4H, -CH$_2$), 6.23–7.76 (m, 16H, CH$_{arom}$), 8.35 (s, 1H, =CH); ^{31}P NMR (298 K, 200 MHz, [D$_8$]THF): $\delta = -9.34$; MS(FAB): *m*/*z*: 549 [*M*]$^+$, 364 [$M - C_{12}H_{11}NO$]$^+$.

Compound 4: A suspension of the macrocycle **1b** (473 mg, 0.15 mmol) in THF (20 mL) was treated with 2,2′-bipyridine (172 mg, 1.1 mmol) dissolved in THF (10 mL) under stirring at room temperature. After 6 h the reaction mixture was filtered, washed with diethyl ether and dried in vacuo to give complex **4**. Yield: 348 mg (87 %); elemental analysis calcd (%) for $C_{23}H_{19}N_3NiO_3$ (444.1): C 62.20, H 4.31, N 9.46, Ni 13.22; found C 61.84, H 4.55, N 9.37, Ni 13.17; IR (Nujol): $\tilde{\nu} = 1603$ (C=C), 1636 (C=O) cm^{-1}; MS(FAB): *m*/*z*: 445 [*M*+H]$^+$, 401 [M+H − CO$_2$]$^+$.

Compound 5: The complex was prepared analogously to **4** using ptmeda instead of bpy. Compound **5** crystallized with THF (0.5 mol). Yield: 407 mg (82 %) for [**5**$\cdot$(THF)$_{0.5}$]; elemental analysis calcd (%) for $C_{24}H_{38}N_4NiO_{3.5}$ (497.29): Ni 11.81; found Ni 11.77; IR (nujol): $\tilde{\nu} = 1578$, 1590 (C=C), 1618 (C=O) cm^{-1}. Single crystals of the solvent free complex **5** suitable for an X-ray structural analysis were grown from dilute THF solutions at −20 °C.

Complex 6: A mixture of **2** (2.35 g 2.49 mmol) and THF (25 mL) was stirred for 2 h, followed by evaporation of 5 mL of the solvent in vacuo. The reaction mixture was filtered over celite and diethyl ether (20 mL) was added to the resulting red solution. Compound **6** was obtained from the mixture at −20 °C as dark-red crystals suitable for X-ray analysis. Yield: 303 mg (34 %); elemental analysis calcd (%) for $C_{74}H_{66}N_6Ni_4O_{10}$ (1434.17): C 61.98, H 4.64, N 5.86, Ni 16.37; found C 61.52, H 4.36, N 5.46, Ni 16.31; IR (Nujol): $\tilde{\nu} = 1573$ (C=C), 1583 (C=O), 1648 (C=N) cm^{-1}.

X-ray crystallography: The intensity data for the compounds were collected with a Nonius KappaCCD diffractometer, using graphite-monochromated Mo$_{K\alpha}$ radiation. Data were corrected for Lorentz and polarization effects, but not for absorption.[26, 27] The structures were solved by direct methods (SHELXS)[28] and refined by full-matrix least squares techniques against F_o^2 (SHELXL-97).[29] For the compounds **1a** (not for the dioxane molecules on the special positions) and **2** the hydrogen atoms were located by difference Fourier synthesis and refined isotropically. The hydrogen atoms of the other structures were included at calculated positions with fixed thermal parameters. All non-hydrogen atoms were refined anisotropically.[30] Only one of the four THF molecules of **1c** could be located and refined. The other three THF molecules are disordered and daubed by the high symmetry (located arounded special positions of $P\bar{3}$). The disorder could not be resolved. The presence of the THF molecules follows from the C,H,N analysis, from GC investigations, from the maxima of difference-Fourier-synthesis and the analogy to **1a** and **1b**. The *R* value could not be enhanced. XP (SIEMENS Analytical X-ray Instruments, Inc.) was used for structure representations.

Crystal data for **1a**:[30] $C_{150}H_{132}N_{12}Ni_6O_{24} \times 4\,C_4H_8O_2$; $M_r = 3191.4$ g mol^{-1}; orange-brown prism; size: 0.22 × 0.20 × 0.12 mm^3, trigonalic; space group: $P\bar{3}$; $a = b = 18.0359(4)$, $c = 13.4557(4)$ Å; $V = 3790.64(16)$ Å^3; $T = -90$ °C; $Z = 1$; $\rho_{calcd} = 1.405$ g cm^{-3}; $\mu(Mo_{K\alpha}) = 8.11$ cm^{-1}; $F(000) = 1672$; 10705 reflections in *h* (−23/23), *k* (−19/19), *l* (−17/17); measured in the range $3.02° \leq \Theta \leq 27.49°$; completeness $\Theta_{max} = 99.7$ %; 5809 independent reflections; $R_{int} = 0.038$; 4262 reflections with $F_o > 4\sigma(F_o)$; 416 parameters; 0 restraints; $R1_{obs} = 0.048$; $wR^2_{obs} = 0.086$; $R1_{all} = 0.081$; $wR^2_{all} = 0.096$; GOF = 1.005; largest difference peak and hole: 0.326/−0.322 e Å^{-3}.

Crystal data for **1b**:[30] $C_{150}H_{132}N_{12}Ni_6O_{24} \times 4\,C_4H_8O$; $M_r = 3127.35$ g mol^{-1}; orange prism; size: 0.32 × 0.30 × 0.28 mm^3, hexagonal; space group $P\bar{3}c1$; $a = b = 17.8840(2)$, $c = 26.9207(4)$ Å; $V = 7456.7(2)$ Å^3; $T = -90$ °C; $Z = 2$; $\rho_{calcd} = 1.361$ g cm^{-3}; $\mu(Mo_{K\alpha}) = 8.18$ cm^{-1}; $F(000) = 3192$; 18509 reflections in *h* (−16/19), *k* (−19/0), *l* (−29/29); measured in the range $3.03° \leq \Theta \leq 23.27°$; completeness $\Theta_{max} = 95.6$ %; 3570 independent reflections; $R_{int} = 0.055$; 3341 reflections with $F_o > 4\sigma(F_o)$; 328 parameters; 0 restraints; $R1_{obs} = 0.036$, $wR^2_{obs} = 0.100$; $R1_{all} = 0.054$; $wR^2_{all} = 0.116$; GOF = 1.030; largest difference peak and hole: 0.286/−0.559 e Å^{-3}.

Crystal data for **1c**:[30] $C_{96}H_{120}N_6Ni_6O_{18}P_6 \times 4\,C_4H_8O$; $M_r = 2472.59$ g mol^{-1}; yellow brown prism; size 0.24 × 0.10 × 0.08 mm^3, trigonalic; space group $P\bar{3}$; $a = b = 27.2930(5)$, $c = 13.7981(3)$ Å; $V = 8901.3(3)$ Å^3, $T = -90$ °C; $Z = 3$; $\rho_{calcd} = 1.303$ g cm^{-3}; $\mu(Mo_{K\alpha}) = 10.76$ cm^{-1}; $F(000) = 3660$; 23636 reflections in *h* (−35/35), *k* (−30/29), *l* (−17/17), measured in the range $2.72° \leq \Theta \leq 27.47°$; completeness $\Theta_{max} = 99.7$ %; 13563 independent reflections; $R_{int} = 0.081$; 8220 reflections with $F_o > 4\sigma(F_o)$; 677 parameters; 0 restraints; $R1_{obs} = 0.119$; $wR^2_{obs} = 0.186$; $R1_{all} = 0.199$; $wR^2_{all} = 0.215$; GOF = 1.108; largest difference peak and hole: 1.505/−0.805 e Å^{-3}.

Crystal data for **2**:[30] $C_{50}H_{44}N_4Ni_2O_8 \times 2\,C_6H_6$; $M_r = 1102.52$ g mol^{-1}; brown prism; size: 0.35 × 0.30 × 0.10 mm^3, triclinic; space group $P\bar{1}$; $a = 10.2749(2)$, $b = 12.3478(4)$, $c = 13.2530(4)$ Å; $\alpha = 96.444(1)$, $\beta = 112.226(2)$, $\gamma = 111.998(2)°$; $V = 1378.59(7)$ Å^3; $T = -90$ °C; $Z = 1$; $\rho_{calcd} = 1.328$ g cm^{-3}; $\mu(Mo_{K\alpha}) = 7.42$ cm^{-1}; $F(000) = 576$; 14703 reflections in *h* (−11/11), *k* (−13/12), *l* (−14/13), measured in the range $2.14° \leq \Theta \leq 23.27°$; completeness $\Theta_{max} = 98.7$ %, 3756 independent reflections; $R_{int} = 0.034$; 3620 reflections with $F_o > 4\sigma(F_o)$; 455 parameters; 0 restraints; $R1_{obs} = 0.032$; $wR^2_{obs} = 0.093$; $R1_{all} = 0.046$; $wR^2_{all} = 0.145$; GOF = 1.007; largest difference peak and hole: 0.329/−0.342 e Å^{-3}.

Crystal data for **3**:[30] $C_{28}H_{31}N_2$ $NiO_4P \times 2\,C_4H_8O$; $M_r = 693.44$ g mol^{-1}; orange-brown prism; size: 0.32 × 0.28 × 0.22 mm^3, triclinic; space group $P\bar{1}$; $a = 8.8146(5)$, $b = 10.7291(6)$, $c = 19.726(1)$ Å; $\alpha = 101.737(3)$, $\beta = 92.430(3)$, $\gamma = 98.376(4)°$; $V = 1802.0(1)$ Å^3; $T = -90$ °C; $Z = 2$; $\rho_{calcd} = 1.278$ g cm^{-3}; $\mu(Mo_{K\alpha}) = 6.28$ cm^{-1}; $F(000) = 736$; 15179 reflections in *h* (−11/11), *k* (−13/13), *l* (−25/25), measured in the range $3.18° \leq \Theta \leq 27.49°$; completeness $\Theta_{max} = 93$ %; 7708 independent reflections; $R_{int} = 0.099$; 6006 reflections with $F_o > 4\sigma(F_o)$; 390 parameters; 0 restraints; $R1_{obs} = 0.111$; $wR^2_{obs} = 0.283$; $R1_{all} = 0.132$; $wR^2_{all} = 0.300$; GOF = 1.120; largest difference peak and hole: 2.096/−1.144 e Å^{-3}.

Crystal data for **5**:[30] $C_{22}H_{34}N_4NiO_3$; $M_r = 461.24$ g mol^{-1}; light yellow prism; size: 0.28 × 0.20 × 0.18 mm^3, monoclinic; space group $P2_1/c$; $a = 9.5129(5)$, $b = 15.7389(9)$, $c = 15.2940(6)$ Å; $\beta = 92.744(3)°$; $V = 2287.2(2)$ Å^3; $T = -90$ °C; $Z = 4$; $\rho_{calcd} = 1.339$ g cm^{-3}; $\mu(Mo_{K\alpha}) = 8.78$ cm^{-1}; $F(000) = 984$; 9346 reflections in *h* (−12/12), *k* (−20/20), *l* (−19/19), measured in the range $3.50° \leq \Theta \leq 27.49°$; completeness $\Theta_{max} = 99.6$ %; 5222 independent reflections; $R_{int} = 0.061$; 3452 reflections with $F_o > 4\sigma(F_o)$; 271 parameters; 0 restraints; $R1_{obs} = 0.049$; $wR^2_{obs} = 0.099$; $R1_{all} = 0.095$; $wR^2_{all} = 0.115$; GOF = 0.986; largest difference peak and hole: 0.352/−0.478 e Å^{-3}.

Crystal data for **6**:[30] $C_{74}H_{66}N_6Ni_4O_{10}$; $M_r = 1434.17$ g mol^{-1}; black prism; size: 0.14 × 0.14 × 0.07 mm^3, monoclinic; space group $P2_1/n$; $a = 13.103(2)$, $b = 12.965(2)$, $c = 19.825(4)$ Å; $\beta = 104.17(2)°$; $V = 3265.4(10)$ Å^3; $T = -90$ °C; $Z = 2$; $\rho_{calcd} = 1.459$ g cm^{-3}; $\mu(Mo_{K\alpha}) = 12.01$ cm^{-1}; $F(000) = 1488$; 7981 reflections in *h* (−14/14), *k* (−14/0), *l* (−22/22), measured in the range $3.19° \leq \Theta \leq 23.37°$; completeness $\Theta_{max} = 98.9$ %; 4603 independent reflections; $R_{int} = 0.1022$; 4603 reflections with $F_o > 4\sigma(F_o)$; 425 parameters; 0 restraints; $R1_{obs} = 0.073$; $wR^2_{obs} = 0.174$; $R1_{all} = 0.118$; $wR^2_{all} = 0.213$; GOF = 0.973; largest difference peak and hole: 0.982/−0.654 e Å^{-3}.

Acknowledgements

We are grateful to the Deutsche Forschungsgemeinschaft (Sonderforschungsbereich 436), the Volkswagenstiftung, and the Fonds der Chemischen Industrie for financial support. C.F. aknowledges the Konrad-Adenauer-Stiftung for a sholarship.

---

[1] B. Dietrich, P. Viout, J.-M. Lehn, *Macrocyclic Chemistry*, VCH, Weinheim, **1993**.

[2] D. S. Lawrance, T. Jiang, M. Levett, *Chem. Rev.* **1995**, *95*, 2229–2260.

[3] J.-M. Lehn, *Supramolecular Chemistry: Concepts and Perspectives*, VCH, Weinheim, **1995**.

[4] D. Philp, J. F. Stoddart, *Angew. Chem.* **1996**, *108*, 1242–1286; *Angew. Chem. Int. Ed. Engl.* **1996**, *35*, 1155–1196, and references therein.

[5] *From Simplicity to Complexity in Chemistry and Beyond* (Eds.: A. Müller, A. Dress, F. Vögtle), Vieweg, Brauschweig, **1996**.

[6] *Transition Metals in Supramolecular Chemistry*, *Perspectives in Supramolecular Chemistry*, *Vol. 5* (Ed.: J.-P. Sauvage), Wiley, **1999**, and references therein.

[7] H. Plenio, *Angew. Chem.* **1997**, *109*, 358–360; *Angew. Chem. Int. Ed. Engl.* **1997**, *36*, 348–351.

[8] Review: I. Haiduc, F. T. Edelmann, *Supramolecular Organometallic Chemistry*, Wiley-VCH, Weinheim, **1999**.

[9] Review: B. J. Holliday, C. A. Mirkin, *Angew. Chem.* **2001**, *113*, 2022–2043; *Angew. Chem. Int. Ed.* **2001**, *40*, 2076–2097.

[10] B. Grossmann, J. Heinze, E. Herdtweck, F. H. Köhler, H. Nöth, H. Schwenk, M. Spiegler, W. Wachter, B. Weber, *Angew. Chem.* **1997**, *109*, 384–385; *Angew. Chem. Int. Ed. Engl.* **1997**, *36*, 387–389.

[11] J. Manna, J. A. Whiteford, P. J. Stang, D. C. Muddimann, R. D. Smith, *J. Am. Chem. Soc.* **1996**, *118*, 1987–1990.

[12] J. Manna, C. J. Kuehl, J. A. Whiteford, P. J. Stang, D. C. Muddimann, S. A. Hofstadler, R. D. Smith, *J. Am. Chem. Soc.* **1997**, *119*, 11611–11619.

[13] S. M. ALQuasi, K. J. Galat, M. Chai, D. G. Ray III, P. L. Rinaldi, C. A. Tessier, W. J. Youngs, *J. Am. Chem. Soc.* **1998**, *120*, 12149–12150.

[14] W. W. Cleland, T. J. Andrews, S. Gutteridge, F. C. Hartman, G. H. Lorimer, *Chem. Rev.* **1998**, *98*, 549–561, and references therein.

[15] a) E. Jabri, M. B. Carr, R. P. Hausinger, P. A. Karplus, *Science* **1995**, *268*, 998–1004; b) P. A. Karplus, M. A. Pearson, R. P. Hausinger, *Acc. Chem. Res.* **1997**, *30*, 330–337.

[16] a) M. M. Benning, J. M. Kuo, F. M. Raushel, H. M. Holden, *Biochemistry* **1994**, *33*, 15001–15004; b) J. L. Vanhooke, M. M. Benning, F. M. Raushel, H. M. Holden, *Biochemistry* **1996**, *35*, 6020–6025.

[17] a) S. Berger, A. Braune, W. Buckel, U. Härtel, M.-L. Lee, *Angew. Chem.* **1996**, *108*, 2259–2261; *Angew. Chem. Int. Ed. Engl.* **1996**, *35*, 2132–2133; b) F. Lynen, J. Knappe, E. Lorch, G. Jütting, E. Ringelmann, J. P. Lachance, *Biochem. Z.* **1961**, *335*, 123–167.

[18] D. Walther, E. Dinjus, J. Sieler, J. Kaiser, O. Lindquist, L. Anderson, *J. Organometal. Chem.* **1982**, *240*, 289–295.

[19] R. Kempe, J. Sieler, D. Walther, J. Reinhold, K. Rommel, *Z. Anorg. Allg. Chem.* **1993**, *619*, 1105–1110.

[20] D. Walther, E. Dinjus, *Z. Chem.* **1981**, *21*, 416–417.

[21] D. Walther, *Coord. Chem. Rev.* **1987**, *79*, 135–174.

[22] D. Walther, S. Geßler, U. Ritter, A. Schmidt, K. Hamza, W. Imhof, H. Görls, J. Sieler, *Chem. Ber.* **1995**, *128*, 281–287.

[23] M. A. Pearson, L. O. Michel, R. P. Hausinger, P. A. Karplus, *Biochemistry* **1997**, *36*, 8164–8172.

[24] D. Walther, C. Fugger, H. Görls, *J. Organometal. Chem.* **2000**, *597*, 116–124.

[25] J. Kliegman, R. K. Barnes, *Tetrahedron* **1970**, *26*, 2555–2560.

[26] COLLECT, Data Collection Software; Nonius B. V., Netherlands, **1998**.

[27] Z. Otwinowski, W. Minor "*Processing of X-Ray Diffraction Data Collected in Oscillation Mode*" in: Methods in Enzymology, *Vol. 276*, Macromolecular Crystallography, Part A (Eds.: C. W. Carter, R. M. Sweet), San Diego Academic Press, **1997**, pp. 307–326.

[28] G. M. Sheldrick, *Acta Crystallogr. Sect. A* **1990**, *46*, 467–473.

[29] G. M. Sheldrick, SHELXL-97 (Release 97-2), University of Göttingen, Germany, **1997**.

[30] Crystallographic data (excluding structure factors) for the structures reported in this paper have been deposited with the Cambridge Crystallographic Data Centre as supplementary publication no. CCDC-140792–140798. Copies of the data can be obtained free of charge on application to CCDC, 12 Union Road, Cambridge CB21EZ, UK (fax: (+44)1223-336-033; e-mail: deposit@ccdc.cam.ac.uk).

Received: July 4, 2001 [F3393]

0947-6539/01/0723-5221 $ 17.50+.50/0